ChemComm

Accepted Manuscript

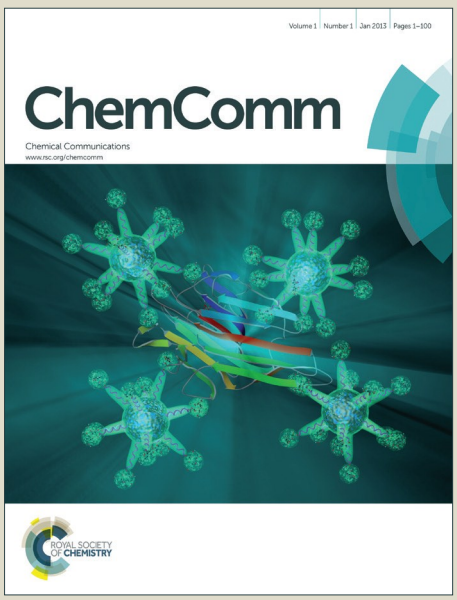

ROYAL SOCIETY OF CHEMISTRY

www.rsc.org/chemcomm

Journal Name

COMMUNICATION

Chondroitin Sulfate Coated Gold Nanoparticles: A New Strategy to Resolve Multidrug Resistance and Thromboinflammation

Received 00th January 20xx,
Accepted 00th January 20xx

DOI: 10.1039/x0xx00000x

www.rsc.org/

Deepanjali Gurav,[ac] Oommen P. Varghese,[a] Osama A. Hamad,[b] Bo Nilsson,[b] Jöns Hilborn,[a] Oommen P. Oommen[a]*

We have developed the first chondroitin sulfate polymer coated gold nanoparticles that can simultaneously overcome mulidrug resistance in cancer cells and suppress thromboinflammation triggered by the chemotherapeutic drug.

Despite advances in cancer treatment, infection, venous thromboembolism, sepsis or drug resistance mediated relapse are the prominent cause of mortality among cancer patients.[1] The root causes for such events are platelets and leukocytes depletion, activation of complement and/or coagulation systems[2] or gradual cancer cell acquisition of cell-surface p-glycoprotein (Pgp), a drug efflux pump, which is encoded by multi drug resistant gene (MDR1).[3] The most common strategies to overcome these challenges are using anti-inflammatory drugs (corticosteroids, dexamethasone etc.),[4] platelet transfusion after each cycle of chemotherapy,[5] using inhibitors of Pgp or knocking down Pgp expression using short interfering RNA or siRNA[3,6] or covalently conjugated drug nanoformulations.[7] However a simple, cost-effective and stable drug delivery system (DDS), which can achieve all the above-mentioned challenges is highly sought-after for anticancer therapy.

In this communication, we present hemocompatible chondroitin sulfate (CS) coated gold nanoparticles (NPs) to deliver antineoplastic drug doxorubicin (DOX) to cancer cells including MDR1 gene expressing DOX resistant cancer cells. Unlike other nanocarriers, which focus on targeted delivery,[8] gold nanoparticles are emerging as a promising agents for anticancer therapy as it functions as a contrast agent, photothermal agent, and radiosensitizer[9] in addition to a drug delivery agent.[10] Our choice of using CS for fabricating gold nanoparticles is based on our previous observation that nanomaterials and bulk hydrogels derived from extracellular matrix components such as hyaluronic acid[11] and CS[12] impart unique biological function. We have therefore utilized such materials for regenerative medicine[13] and drug delivery applications.[14]

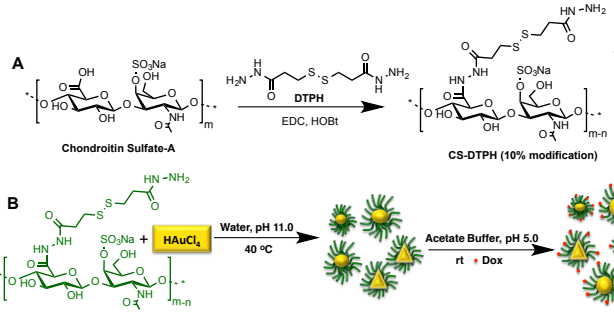

Figure 1. (A) Scheme for the synthesis of CS-DTPH. (B) Schematic representation of CS-Au-NP synthesis from 3,3'-dithiobis(propanoic hydrazide) modified CS.

To design CS coated NPs, we first synthesized CS derivative bearing a disulfide group and free hydrazide unit. We envisioned that disulfide groups would co-ordinate gold (Au^0) while free hydrazide moiety could be used as a handle for conjugating drug molecules. For this purpose, we modified CS with 10% hydrazide group using 3,3'-dithiobis(propanoic hydrazide) or DTPH following carbodiimide coupling chemistry as previously optimized in our group[15] (Figure 1). This modified CS function both as a reducing agent and as a surface-capping agent for the gold NP preparation. To design gold NP of the desired size we tested different ratios of $HAuCl_4$ and CS-DTPH at 40 °C. After careful evaluation, a ratio of 3 molar equivalents of CS-DTPH (with respect to disaccharide units) and 1 molar equivalents of $HAuCl_4$ was chosen, resulting in particles with average size of 80 nm and a narrow size distribution and as observed by dynamic light scattering (DLS) (Table S1, Supporting Information or SI). Interestingly, the lyophilization and re-dispersion of particles in water delivered uniform particles with an average size of 98 nm. This suggests that there is no significant aggregation of the particles as a result of lyophilization procedure (Figure 2A). We termed this CS coated

[a] *Department of Chemistry, Ångström Laboratory Uppsala University, SE-75121, Sweden E-mail: oommen.op@kemi.uu.se Address here.*
[b] *Department of Immunology, Genetics and Pathology, Rudbeck Laboratory, Uppsala University, SE-75105, Sweden*
[c] *Department of Chemistry, Savitri Bai Phule Pune University, Maharashtra, India*

† Electronic Supplementary Information (ESI) available: Materials and methods, synthesis protocol, details on stability studies, FACS studies, haematological studies and cytotoxicity studies are provided. See DOI: 10.1039/x0xx00000x

NPs as CS-Au-NP. The free hydrazide residue of CS-Au-NP was utilized for conjugating a clinically used anticancer drug DOX via acid-labile hydrazone linkage at C-13 position as previously reported.[14] Such a drug conjugation strategy would facilitate selective release of the drug at the acidic tumor microenvironment. The DOX conjugated CS-Au-NP was termed as CS-Au-DOX, which was extensively dialyzed and stored as lyophilized material. Re-dispersion of this material in water resulted in NPs of ≈80 nm size by DLS measurement (Figure 2B). The polyanionic coating of these particles was also confirmed by the zeta potential (ζ) measurements, which showed a negative ζ for CS-Au-NP and CS-Au-DOX to -52.7 and -56.8 respectively (Figure 2C and 2D).

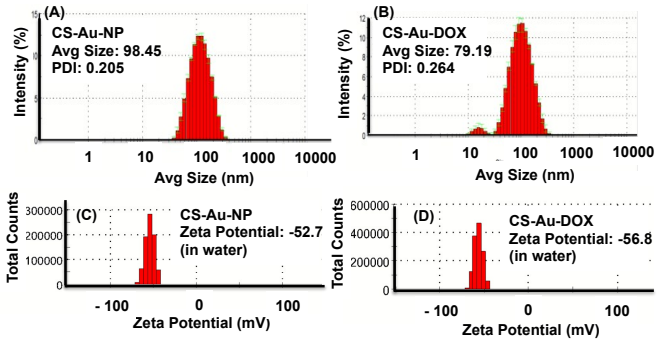

Figure 2. (A,B) Dynamic light scattering profile and (C, D) Zeta Potential of CS-Au-NP and CS-Au-DOX. (C,D) UV-VIS spectra of nanoparticle before and after DOX loading. (D) SEM image of CS-Au-NP.

The UV studies of CS-Au-NP showed an absorbance at 540 nm and an NIR absorbance at longer wavelength (~1000 nm, Figure 3A). This NIR plasmon absorption may be advantageous for diagnostic and biomedical applications as living tissues show minimum absorption at this wavelength. The UV studies of CS-Au-DOX revealed that, upon DOX conjugation and lyophilization, the planar species got disrupted and the NIR absorbance shifted from ~1000 nm to ~750nm (Figure 3A). The reduction in size upon DOX conjugation of CS-Au-NP (from 98 nm to 80 nm, as observed by DLS measurement) could be attributed to this effect. The DOX loading in these particles was estimated to be 6.27 weight% by UV spectroscopy, which corresponds to 62.7% drug loading efficiency relative to the feed ratio.

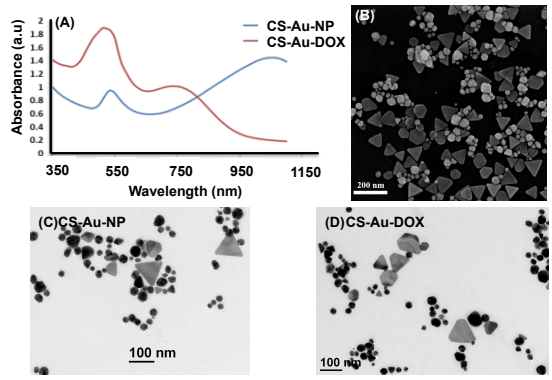

Figure 3. (A) UV-VIS spectra of nanoparticle before and after DOX loading (B) SEM image of CS-Au-NP. (C, D) TEM image of CS-Au-NP and CS-Au-DOX.

Interestingly, the scanning electron microscopy (SEM) analysis of re-dispersed NPs showed predominantly triangular shape with some smaller spherical particles (Figure 3B). We do not know the cause for the anisotropic growth of the Au-NP in presence of CS-DTPH. The TEM analysis of CS-Au-NP and CS-Au-DOX did not show any significant differences (Figure 3C-3D). The ^{1}H NMR analysis of CS-Au-NP demonstrated a chemical shift δ = 3.19 ppm for methylene –CH_2S– protons in Au-NP, which is nearly 0.2–0.4 ppm downfield as compared to that of CS-DTPH (δ = 3.01 ppm) or thiol modified CS respectively (CS-SH; δ = 2.81 ppm; H_a in Figure 3). The splitting pattern of this methylene proton also resolved to a sharp triplet with coupling constant J = 7.3 Hz, which is considerably different from CS-SH (Figure 4C). This NMR pattern is consistent with the reported literature[16] and implies that all the disulfide groups are effectively complexed to the gold surface. Of note, native CS did not form NPs under optimized condition, albeit, in the presence of reducing agents.[17]

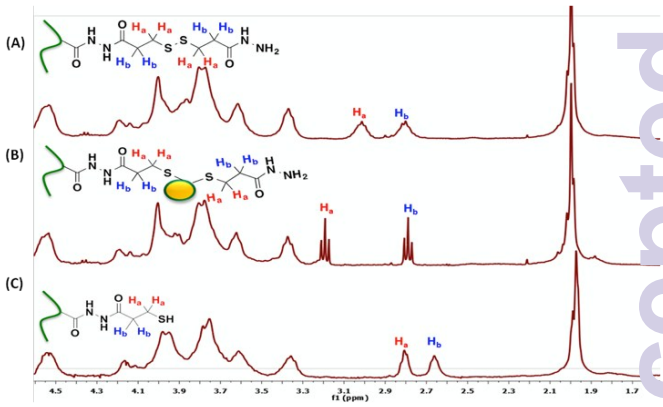

Figure 4. (A) 1H NMR spectrum of CS-DTPH, (B) CS-Au-NP, and (C) CS-SH in D2O at 25 °C.

We further evaluated the stability of CS-Au-NP in phosphate buffer saline (PBS) at pH 5.0, pH 7.4 and PBS pH 7.4 containing 20% fetal bovine serum (FBS) for 72 h (Figure S1 and Table S2 in SI). Under these conditions, the size of the NPs also did not change even after 72 h incubation at 25 °C. This demonstrates that polyanionic coating of gold surface enhances NP stability even in presence of serum and NaCl (140 mM) (Table S2 in SI).

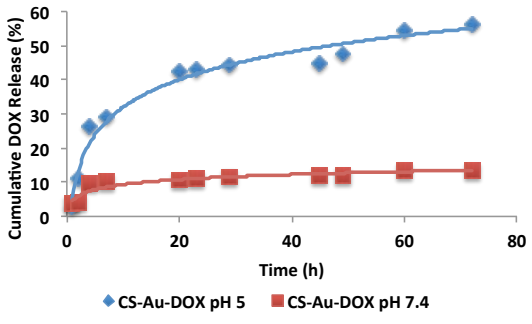

Figure 5. Release kinetics of DOX from CS-Au-DOX at pH 5.0 and pH 7.4 at 37 °C

In order to elucidate pH responsive drug release, we performed the DOX release experiment following dialysis method at physiological pH (pH 7.4) and at lysosomal pH (pH 5) for 72 h at 37 °C to mimic the in vivo scenario. Indeed, CS-Au-DOX showed only 13% DOX release in 72h with near zero-order kinetics at pH 7.4, while 56% was released at lysosomal pH (Figure 4).

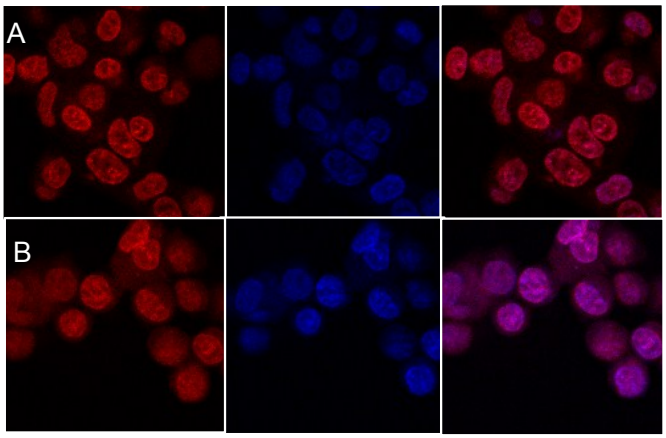

Figure 6. CLSM images of intracellular DOX localization with (A) free DOX or (B) CS-Au-DOX in HCT116 cells, after 4 h incubation. The panel images from left to right show DOX fluorescence in cells (red), cell nuclei stained by DAPI (blue), and overlays of two images.

We further performed cytotoxicity studies of DOX and CS-Au-DOX in human colon carcinoma cell lines HCT116, GP5D, human ovarian carcinoma cell line A2780 and its DOX resistant variant A2780-Adr, expressing high Pgp levels (Figure S2 in SI). The cytotoxic evaluations were performed using ApoTox-Glo™ Triplex Assay. We utilized this assay to estimate the inhibition coefficient with 50% cell death (IC_{50}) upon CS-Au-DOX and free DOX treatment. Surprisingly, these experiments revealed that CS-Au-DOX were more toxic than free drug in all cell lines tested (Table 1 and Figure S3 in SI).

Table 1. Cytotoxicity study in different mammalian cell lines

Cell Lines	DOX IC50 (nM)[a]	CS-Au-DOX IC50 (nM)[a]	Fold Increase in activity[b]
GP5D	156.30	125.60	1.24
HCT116	218.77	165.95	1.32
A2780	204.17	67.29	3.08
A2780-Adr	1288.25	67.29	19.14

[a]50% inhibition coefficient in nanomolar concentrations; [b]fold increase in cytotoxicity with respect to doxorubicin

Gratifyingly, we observed significantly higher toxicity (≈19-folds) in DOX resistant A2780-Adr cells as compared to free DOX. Notably, the IC_{50} values of DOX and CS-Au-DOX were identical in both A2780 and A2780-Adr cell lines. This indicates that our NP formulation could overcome the effects of drug-efflux pump, making them ideal candidate for treating MDR1 expressing tumor. The CS-Au-NP did not show any cytotoxicity under these concentrations (data not shown). We also corroborated our toxicity results using confocal laser scanning microscope (CLSM) in HCT116 cells. The confocal images clearly showed that CS-Au-DOX is efficiently internalized and translocated into the nucleus of HCT116 cells (Figure 6).

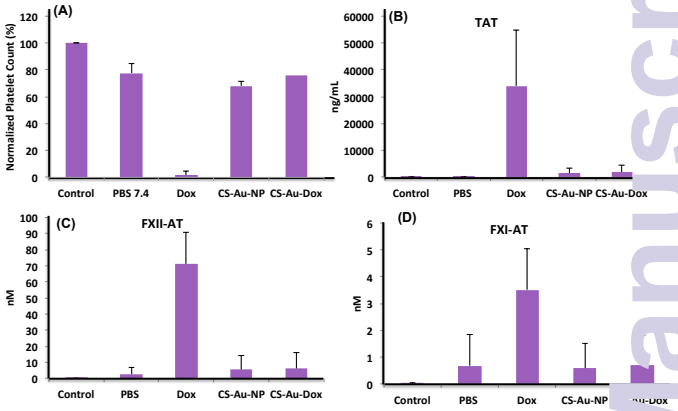

Figure 7. (A) Platelet count, (B) thrombin-antithrombin complex levels, (C) FXIIa-antithrombin complex levels, (D) FXIa-antithrombin complex levels in presence of DOX, CS-Au-DOX and CS-Au-NP.

Chemotherapeutic agents and nanoparticles are generally evaluated in immune compromised mice assuming that the cytotoxic drugs are generally immunosuppressive.[18] Recent evidence on NP-blood interaction studies revealed that several NPs by themselves trigger coagulation and complement activation, which in turn activates tumor growth.[19,20] Since mice and humans have significant differences in the innate and adaptive immunity,[21] an ex-vivo human based system is greatly needed to screen the efficacy of drugs in humans. We performed hematological studies of DOX and CS-Au-DOX using the ex-vivo Chandler loop model with some modifications. The tubings and the materials used in this experiments were coated with heparin, such that it mimics the endothelial wall of our blood vessel. The walls of our blood vessel are covered with a film of heparan sulphate, the glycocalyx; a heparin-like molecule, that protects the streaming blood from clotting. This technique allows us to test NPs and drugs in contact with blood without using any anticoagulant that could skew the results during testing. We evaluated the platelet aggregation and activation of the inflammatory response by the enzyme-linked immunosorbent assay (ELISA) using fresh non-anticoagulated human whole blood. We observed a marked drop in platelet count and macroscopic clotting when blood was incubated with 60 μM DOX for 60 min at 37 °C. Conversely, such adverse effect was absent in CS-Au-DOX group (with 60 μM equivalent DOX) or CS-Au-NP. This indicates that DOX induced acute platelet toxicity, which is suggested to induce thrombocytopenia in DOX treated patients,[23] could be circumvented using our nanoformulations (Figure 7A). Thereafter, we measured thrombin-antithrombin (TAT) complex formation, which is a marker of coagulation activation. TAT levels are unregulated in most cancer patients such as in acute lymphatic leukemia patients.[24] In our experiments, we observed that DOX significantly triggered the

coagulation parameter (TAT complex), which was markedly attenuated in presence of CS-Au-DOX. (Figure 7B).

To further probe the role of DOX and nanocarrier for activation of blood clotting, we measured Factor XII (FXII) and Factor XI (FXI), the key regulators of this activation (Figure 7C, 7D). Antithrombin (AT) and C1-inhibitor (C1INH) are the most important inhibitors that form complexes with FXII and FXI. The formation of FXIIa-AT complex and FXIa-AT complex is believed to be specific for clotting and fibrin generation, whereas FXIIa-C1INH complex and FXIa-C1INH complex are indicative of material-induced blood clotting.[25] We measured FXIIa-AT, FXIa-AT, FXIIa-C1INH and FXIa-C1INH complex levels in presence of free DOX and CS-Au-DOX. These experiments revealed that DOX itself increases FXIIa-AT and FXIa-AT levels which is negated by CS-Au-DOX (Figure 7C, 7D). Negligible levels of FXIIa-C1INH and FXIa-C1INH were detected in all samples (data not shown). Hence, free DOX have detrimental effect on platelets and also trigger coagulation cascade, which can be prevented using our NP formulation strategy. Since thrombotic complication occurs in ≈50% of cancer patients undergoing chemotherapy,[26] and typically ovarian cancer patients experience disease relapse within 2 years of the initial chemotherapy,[27] our findings will open new avenues for developing innocuous DDS for such tumours with minimal side effects. Our Au-NP design is simple, scalable, and storable as a lyophilized material, which are essential criteria for any drug formulations.

This work was supported by grants from Swedish Strategic Research 'StemTherapy' and European Community's Seventh Framework Programme project 'DIREKT' 602699. We acknowledge Scilife platform of Karolinska high-throughput center, Dr. Jianping Liu for cytotoxicity studies, Dr. Sandeep Kadekar for confocal analysis, and Dr. Anumol Ashokkumar for SEM analysis. We thank Dr. Biswarup Satpati from Saha Institute of Nuclear Physics, India for TEM analysis.

Notes and references

1 (a) A. A. Khorana, C. W. Francis, E. Culakova, N. M. Kuderer, G. H. Lyman, *J. Thromb. Haemost*. 2007, **5**, 632–634; (b) P. Ferroni, S. Riondino, F. Guadagni, M. Roselli, *Haematologica*, 2013, **98**, e153-e154

2 S.-H. Kim, K.-M. Lim, J.-Y. Noh, K. Kim, S. Kang, Y. K. Chang, S. Shin, J.-H. Chung, *Toxicol. Sci.* 2011, **124**, 215–224.

3 G. Szakács, J. K. Paterson, J. A. Ludwig, C. Booth-Genthe, M. M. Gottesman, *Nature Rev*. 2006, **5**, 219–234.

4 R. E. Coleman, *Biotherapy*, 1992, **4**, 37–44.

5 C. A. Schiffer, K. C. Anderson, C. L. Bennett, S. Bernstein, L. S. Elting, M. Goldsmith, M. Goldstein, H. Hume, J. J. McCullough, R. E. McIntyre, B. L. Powell, J. M. Rainey, S. D. Rowley, P. Rebulla, M. B. Troner, A. H. Wagnon, *J. Clin. Oncol*., 2001, **19**, 1519–1538.

6 X. Yang, A. K. Iyer, A. Singh, E. Choy, F. J. Hornicek, M. M. Amiji, Z. Duan, *Sci. Rep*. 2015, **5**, 1–9.

7 (a) R. Qi, H. Xiao, S. Wu, Y. Li, Y. Zhang, X. Jing, *J. Mater. Chem. B*, 2015, **3**, 176-179; (b) H. Song, W. Li, R. Qi, L. Yan, X. Jing, M. Zheng, H. Xiao, *Chem. Commun*., 201[illegible] **51**, 11493-11495.

8 E. Gullotti, Y. Yeo, *Mol. Pharm*., 2009, **6**, 1041-1051

9 S. Jain, D. G. Hirst, J. M. O'Sullivan, *Br. J. Radiol*. 2012, **85**, 101–113.

10 T. L. Doane, C. Burda, *Chem. Soc. Rev*. 2012, **41**, 2885-2911

11 O. P. Varghese, W. Sun, J. Hilborn, D. A. Ossipov, *J. Am Chem. Soc*. 2009, **131**, 8781–8783.

12 H. Yan, O. P. Oommen, D. Yu, J. Hilborn, H. Qian, O. P. Varghese, *Adv. Funct. Mat*. 2015, **25**, 3907–3915.

13 O. P. Oommen, S. Wang, M. Kisiel, M. Sloff, J. Hilborn, O. P. Varghese, *Adv. Funct. Mat*. 2013, **23**, 1273–1280.

14 O. P. Oommen, J. Garousi, M. Sloff, O. P. Varghese, *Macromol. Biosci*. 2014, **14**, 327–333.

15 S. Wang, O. P. Oommen, H. Yan, O. P. Varghese, *Biomacromol.* 2013, **14**, 2427–2432.

16 F. Porta, Z. Krpetic, L. Prati, A. Gaiassi, G. Scari, *Langmuir* 2008, **24**, 7061-7064.

17 M. Tengdelius, D. Gurav, P. Konradsson, P. Påhlsson, M. Griffith, O. P. Oommen, *Chem. Commun*. 2015, **51**, 8532–8535.

18 R. A. Lake, B. W. S. Robinson, *Nat. Rev. Cancer* 2005, [illegible], 397 –405.

19 A. N Ilinskaya, M. A. Dobrovolskaia, *Nanomedicine* 2013, **8**, 969–981.

20 S. M. Moghimi, *J. Control. Rel*. 2014, **190**, 556–562.

21 K. N. Ekdahl, J. Hong, O. A. Hamad, R. Larsson, B. Nilsson, *Adv. Exp. Med. Biol*. 2013, **735**, 257–270.

22 J. Mestas, C. C. W. Hughes *J. Immunol*. 2004, **172**, 2731–2738

23 E. J. Kim, K. M. Lim, K. Y. Kim, O. N. Bae, J. Y. Noh, S. M Chung, S. Shin, Y. P. Yun, J. H. Chung, *J. Thromb. Haemost.* 2009, **7**, 1172–1183.

24 K. Chojnowski, E. Wawrzyniak, J. Trelinski, J. Niewiarowska, C. Cierniewski, *Leuk. Lymphoma* 1999, **36**, 77–84

25 J. Bäck, C. Lood, A. A. Bengtsson, K. N. Ekdahl, B. Nilsson, *Arthritis Res. Ther.* 2013, **15**, R206–216.

26 S. Kvolik, M. Jukic, M. Matijevic, K. Marjanovic, L. Glavas-Obrovac, *Surg. Oncol.* 2010, **19**, e33–e46.

27 R. Agarwal, S. B. Kaye, *Nat Rev. Cancer* 2003, **3**, 502–516.